MOLECULAR AND CELLULAR BIOLOGY, Sept. 2004, p. 7548–7558 Vol. 24, No. 17
0270-7306/04/$08.00+0 DOI: 10.1128/MCB.24.17.7548–7558.2004

Neonatal Lethality, Dwarfism, and Abnormal Brain Development in *Dmbx1* Mutant Mice

Akihira Ohtoshi and Richard R. Behringer*

Department of Molecular Genetics, M. D. Anderson Cancer Center, University of Texas, Houston, Texas

Received 17 October 2003/Returned for modification 18 January 2004/Accepted 30 May 2004

***Dmbx1* encodes a *paired*-like homeodomain protein that is expressed in developing neural tissues during mouse embryogenesis. To elucidate the in vivo role of *Dmbx1*, we generated two *Dmbx1* mutant alleles. *Dmbx1*$^-$ lacks the homeobox and *Dmbx1*^{z} is an insertion of a *lacZ* reporter gene. *Dmbx1*^{z} appears to be a faithful reporter of *Dmbx1* expression during embryogenesis and after birth. *Dmbx1-lacZ* expression was detected in the superior colliculus, cerebellar nuclei, and subpopulations of the medulla oblongata and spinal cord. Some *Dmbx1* homozygous mutant mice died during the neonatal period, while others survived to adulthood; however, their growth was impaired. Both heterozygous and homozygous mutant offspring from *Dmbx1* homozygous mutant females exhibited a low survival rate and poor growth. However, even wild-type pups fostered onto *Dmbx1* homozygous mutant females grew poorly, suggesting a *Dmbx1*-dependent nursing defect. *Dmbx1* mutant mice had an aberrant *Dmbx1-lacZ* expression pattern in the nervous system, indicating that they had abnormal brain development. These results demonstrate that *Dmbx1* is required for postnatal survival, growth, and brain development.**

The central nervous system (CNS) is derived from the neural plate, a tissue that arises from the anterior epiblast of the mouse gastrula (28). Complex morphogenetic processes transform the relatively flat neural plate into the neural tube. By the time the neural tube is formed, it has differentiated morphological segments along the anterior-posterior axis and is divided into several compartments called neuromeres. The neuromeres in the forebrain and hindbrain comprise six prosomeres and eight rhombomeres, respectively. This segmentation is induced and maintained by the expression of segment-specific genes, including homeobox genes that encode homeodomain-containing transcription factors.

The homeodomain is a conserved DNA-binding motif that consists of ~60 amino acid residues. The homeoproteins are divided into two groups, clustered and dispersed, according to how they are distributed on the chromosomes. Mammals have four *Hox* gene clusters. Homeobox genes belonging to the dispersed class are further divided into several subclasses, primarily by the homeodomain sequences.

There are many homeobox genes that are known to be expressed in developing brains and/or mature nervous systems in mice (32). Several *Hox* genes are expressed in specific rhombomeres and are required for the identification of neuromeres. In the forebrain, several dispersed-class homeobox genes that belong to *Dlx*, *Emx*, *Nkx*, and *paired*-like subclasses are expressed in region-specific patterns. Based on the restricted expression pattern of regulatory genes and morphological observations, a prosomeric model of forebrain patterning was proposed (27). The embryonic midbrain is a compartment structure located between the forebrain and hindbrain and can be considered one of the neuromeres. *Otx* genes are expressed in the embryonic midbrain and mark the midbrain-hindbrain boundary.

To date, >30 *paired*-like homeoproteins have been identified in mice, and about two-thirds of them are involved in the induction or formation of neural tissues, as well as neuronal cell-type specification. For example, *Otx1* is required for axonal projections of cortical neurons (36). *Otx2* is essential for anterior neuroectoderm specification (1, 3, 17). *Phox2a* and *Phox2b* are essential for the development of adrenergic neurons (20, 25). *Prop1* is required for the differentiation of pituitary lineage cells, and its functional deficiency causes Ames dwarfism in mice (29).

A novel *paired*-like homeobox gene, *Dmbx1*, expressed in neural tissues of the developing mouse embryo, was recently identified (24). *Dmbx1* expression was initially detected at embryonic day 7.5 (E7.5) in the anterior head folds, and by E8.5, expression was detected in the prospective midbrain region. Between E9.5 and E10.5, the midbrain expression was maintained, and in addition, the expression was detected in the caudal diencephalon (prosomere 1) and nasal pits. At later stages of embryogenesis, subregions of the hindbrain and a subset of spinal cord neurons also expressed *Dmbx1* (4). *Dmbx1* orthologues have also been identified in other vertebrates, including chicken and zebrafish (8, 10). As in the mouse, chicken and zebra fish *Dmbx1* expression was also detected in the midbrain and pretectum. A gene knockdown study using antisense oligonucleotides indicated that zebra fish *Dmbx1* (*mbx*) is important for the development of the eyes and tectum (10).

To investigate the in vivo function of mouse *Dmbx1*, we generated two mutant alleles of *Dmbx1*, including a homeobox deletion (*Dmbx1*$^-$) and a *lacZ* insertion (*Dmbx1*^{z}). Here, we show that *Dmbx1* is important for nervous system development, neonatal survival, postnatal growth, and nursing ability.

* Corresponding author. Mailing address: Department of Molecular Genetics, University of Texas, M. D. Anderson Cancer Center, 1515 Holcombe Blvd., Houston, TX 77030. Phone: (713) 794-4614. Fax: (713) 794-4394. E-mail: rrb@mdanderson.org.

MATERIALS AND METHODS

Generation of *Dmbx1* mutant mice. A mouse 129/SvEv strain genomic library was screened to isolate *Dmbx1* genomic DNA using a previously reported *Dmbx1*

homeobox probe (24). To generate the *Dmbx1*$^-$ allele, we used 4.4-kb HindIII and 2.6-kb BglII genomic DNA fragments as the 5′ and 3′ homologous arms for a targeting vector, respectively. We replaced a ~1.9-kb HindIII-BglII genomic sequence encoding the entire homeodomain and adjacent intron sequences with a floxed Neo cassette (Fig. 1A). To construct a *Dmbx1*^{z} targeting vector, we inserted a splice acceptor (SA)-internal ribosomal entry sequence (IRES)-*lacZ*-floxed Neo cassette into a StuI site located in intron 1 of a 5.8-kb XbaI genomic fragment (Fig. 1E). The *lacZ* sequence included a nuclear localization signal. Both targeting vectors have a herpes simplex virus thymidine kinase expression cassette located on the 3′ arms of homology for negative selection. Twenty-five micrograms of linearized targeting vector (Fig. 1A and E) were electroporated into 10^7 protamine-Cre (PC3) ES cells (22). After 10 days of drug selection with 350 μg of G418/ml and 200 μM FIAU [1-(2′-deoxy-2′-fluoro-β-D-arabinofuranosyl)-5-iodouracil], ES cell colonies were picked and genotyped. Correctly targeted ES cell clones were injected into blastocysts from C57BL/6 (B6) mice and transferred into pseudopregnant females. The resulting chimeric male mice were mated with B6 females for germ line transmission of the *Dmbx1* targeted alleles. Two independent ES cell clones were confirmed to be germ line transmitted for both *Dmbx1*$^-$ and *Dmbx1*^{z} alleles. All mice were examined on a B6-129 mixed genetic background. A 5′ probe used for Southern analysis was PCR amplified using the primers 5′-TTC CAG ACC CTG GTG TTA G-3′ and 5′-GAT TAA ACA TAC ATG CAA TGT G-3′. A 0.2-kb HindIII-BglII fragment was used as a 3′ probe. The PCR primers used for genotyping were as follows: a, 5′-AAA CAA CGT CGG AGT CGC-3′; b, 5′-ATC TTC TGG GGC AGA CTC-3′; c, 5′-CCT TTC CCA TGT GCT GTG-3′; d, 5′-GTT CCA GGA CAG CTT GGG-3′; e, 5′-AAG TAC TGG AGC GTC TGG GGA TT-3′; and f, 5′-CTG ACC AGG AGG ACA ACC GAA G-3′. The PCR conditions were 94°C for 2 min 30 s, followed by 35 cycles of 94°C for 30 s, 55°C for 1 min, and 72°C for 1 min, and a final extension of 72°C for 10 min.

β-Galactosidase staining and histological analysis. Embryos and brains were stained for β-galactosidase activity as described previously (23). Seven-micrometer-thick paraffin-embedded tissue sections were cut and stained with hematoxylin and eosin Y or cresyl violet. Antibodies used for immunostaining were anti-growth hormone (anti-GH) and anti-thyroid-stimulating hormone (anti-TSH), obtained from the National Hormone and Peptide Program, and anti-neurofilament, 2H3, obtained from the Developmental Studies Hybridoma Bank, Iowa City, Iowa. Immunological reactions were visualized using a Vector ABC kit or by peroxidase-diaminobenzidine reaction.

Section in situ hybridization and Northern analysis. Twelve-micrometer-thick paraffin sections were prepared and hybridized with a digoxigenin (Dig) 11-UTP-labeled anti-sense or sense (control) *Dmbx1* homeobox probe (24). After being washed in SSC buffer (1× SSC is 0.15 M NaCl plus 0.015 M sodium citrate), the sections were incubated with alkaline phosphatase-conjugated anti-Dig-11-UTP antibodies (Roche) and visualized using nitroblue tetrazolium and BCIP (5-bromo-4-chloro-3-indolylphosphate) as substrates. Northern analysis was performed using a filter purchased from ORIGENE hybridized with a *Dmbx1* homeobox probe (24).

RESULTS

Generation of *Dmbx1* mutant mice. We generated two targeted *Dmbx1* mutant alleles, *Dmbx1*$^-$ and *Dmbx1*^{z}, by homologous recombination in the PC3 mouse ES cell line, which is homozygous for a *Prm1-Cre* transgene (Fig. 1B and F). *Dmbx1*$^-$ lacks the second and third exons, which encode the homeodomain. *Dmbx1*^{z} is an insertional mutation of a SA-IRES-*lacZ* cassette into intron 1. Correctly targeted ES cell clones were injected into blastocysts to generate chimeric mice that transmitted the targeted mutations to their offspring. When PC3 ES cells differentiate into spermatids in male chimeras, Cre recombinase will be expressed, causing the floxed Neo cassettes in the *Dmbx1* targeted loci to be removed prior to the fertilization of oocytes (Fig. 1). Mice heterozygous for the *Dmbx1*$^-$ and *Dmbx1*^{z} alleles appeared normal and were fertile.

***Dmbx1-lacZ* expression in the CNS.** We examined *lacZ* expression in *Dmbx1*^{z} heterozygous mutant mice (*Dmbx1*$^{z/+}$). At E8.5, *lacZ* expression was detected in the prospective midbrain region, and later, at E9.5 and E10.5, *lacZ* expression was detected in the caudal diencephalon, midbrain, and nasal pits (Fig. 2A to C). At E12.5 and E14.5, in addition to the above-mentioned regions, subregions of the hindbrain and spinal cord expressed *lacZ* (Fig. 2D to F). These expression sites are similar to the previously reported *Dmbx1* mRNA expression pattern detected by whole-mount in situ hybridization, indicating that the *Dmbx1*^{z} allele recapitulates the endogenous *Dmbx1* expression pattern and may be a useful marker to identify potential *Dmbx1* expression sites.

We also examined *Dmbx1-lacZ* expression in the postnatal CNS. At postnatal day 7 (P7), *lacZ* expression was detected in the tectum of the midbrain and subregions of the medulla oblongata, cerebellum, and spinal cord (Fig. 2G and H). In the midbrain at P21, the superior colliculus was positively stained, while staining of the inferior colliculus was absent (Fig. 2I and data not shown). Histological analyses revealed that the *Dmbx1-lacZ*-expressing cells were primarily located in the superficial layer of the superior colliculus (Fig. 2J). *Dmbx1-lacZ* expression was also detected in deep nuclei of the cerebellum, medulla oblongata, and spinal cord (Fig. 2K to M). Cresyl violet staining demonstrated that these *Dmbx1-lacZ*-expressing cells had relatively large nuclei, suggesting that the cells were neurons (Fig. 2N to Q). *Dmbx1* mRNA expression was detected in the superior colliculus at P19 by section in situ hybridization (Fig. 2R and S). Northern analysis showed that *Dmbx1* is expressed in the adult brain (Fig. 2T). These results indicate that *Dmbx1-lacZ* expression is consistent with the endogenous *Dmbx1* expression pattern in the postnatal CNS.

Neonatal lethality and growth defects of *Dmbx1* mutant mice. To examine the in vivo role of *Dmbx1*, we generated *Dmbx1* homozygous mutant mice by intercrossing *Dmbx1* heterozygotes. Pups obtained from *Dmbx1*$^-$ heterozygous (*Dmbx1*$^{+/-}$) mutant intercrosses were initially genotyped at P9. Only 13.0% of the progeny were *Dmbx1*$^-$ homozygous (*Dmbx1*$^{-/-}$) mutants, which was significantly lower than the expected Mendelian ratio (Table 1). However, at E18.5, the ratio of wild-type, *Dmbx1*$^{+/-}$, and *Dmbx1*$^{-/-}$ mice was nearly the expected Mendelian ratio. These results suggest that some *Dmbx1*$^{-/-}$ mice died postnatally before P9. Similar results were obtained when *Dmbx1*$^{+/z}$ mice were intercrossed (Table 1). This indicates that the insertion of the SA-IRES-*lacZ* cassette disrupts *Dmbx1* function and that the *Dmbx1*^{z} allele behaves phenotypically like the *Dmbx1*$^-$ allele.

Those *Dmbx1* homozygous mutant mice that did survive were consistently smaller than their heterozygous and wild-type littermates. Therefore, we measured body weights at P7, P14, and P21 (Fig. 3A). *Dmbx1*$^{-/-}$ mice were significantly lighter in weight than wild-type or *Dmbx1*$^{+/-}$ mice and were proportionally smaller. However, body weights at E18.5 and P0 were similar among wild-type, *Dmbx1*$^{+/-}$, and *Dmbx1*$^{-/-}$ mice, indicating that the observed growth defect is a postnatal event (Fig. 3B). The growth impairment of *Dmbx1*$^{-/-}$ mice continued throughout adulthood, although growth rates were comparable to those of wild-type or *Dmbx1*$^{+/-}$ mice after weaning (data not shown). The growth defect was also observed in *Dmbx1-lacZ* homozygous mutant (*Dmbx1*$^{z/z}$) mice, confirming the functional similarity between the *Dmbx1*$^-$ and *Dmbx1*^{z} alleles (Fig. 3C).

We observed little or no milk in the stomachs of *Dmbx1*

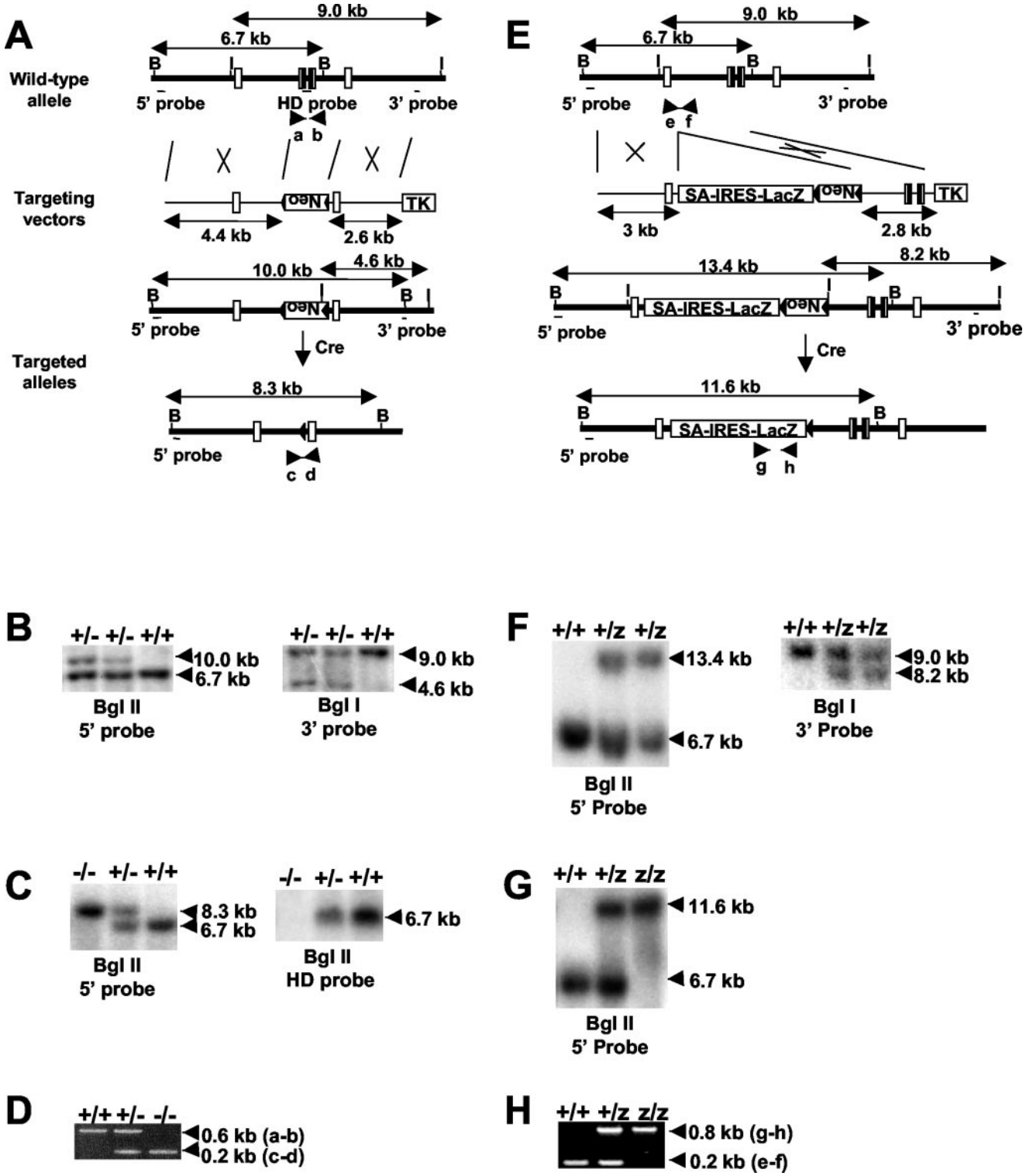

FIG. 1. Generation of *Dmbx1* targeted mice. (A and E) Strategies to generate *Dmbx1*$^-$ and *Dmbx1*^{z} alleles are shown. *Dmbx1* consists of four coding exons (boxes). To generate the *Dmbx1*$^-$ allele, the second and third coding exons encoding the homeodomain (solid boxes) was replaced by a floxed Neo cassette as described in Materials and Methods. For the generation of the *Dmbx1*^{z} allele, an SA-IRES-*lacZ*-floxed Neo cassette was inserted into an intron between the first and second coding exons. Solid triangles, *loxP* sequences; TK, thymdine kinase gene for negative selection; Neo, neomycin resistance gene for positive selection; LacZ, *lacZ* gene containing a nuclear localization signal; Cre, Cre recombinase. Essential diagnostic restriction enzyme sites are indicated by vertical bars. B, BglII; I, BglI. Positions of probes used for Southern analysis and PCR primers (see Materials and Methods) are indicated by horizontal bars and arrowheads, respectively. (B and F) Southern analyses of ES cell DNA. +, wild-type allele; −, *Dmbx1*$^-$ allele; z, *Dmbx1*^{z} allele. (C and G) Genotyping of *Dmbx1* targeted mice. (D and H) PCR genotype of *Dmbx1* targeted mice.

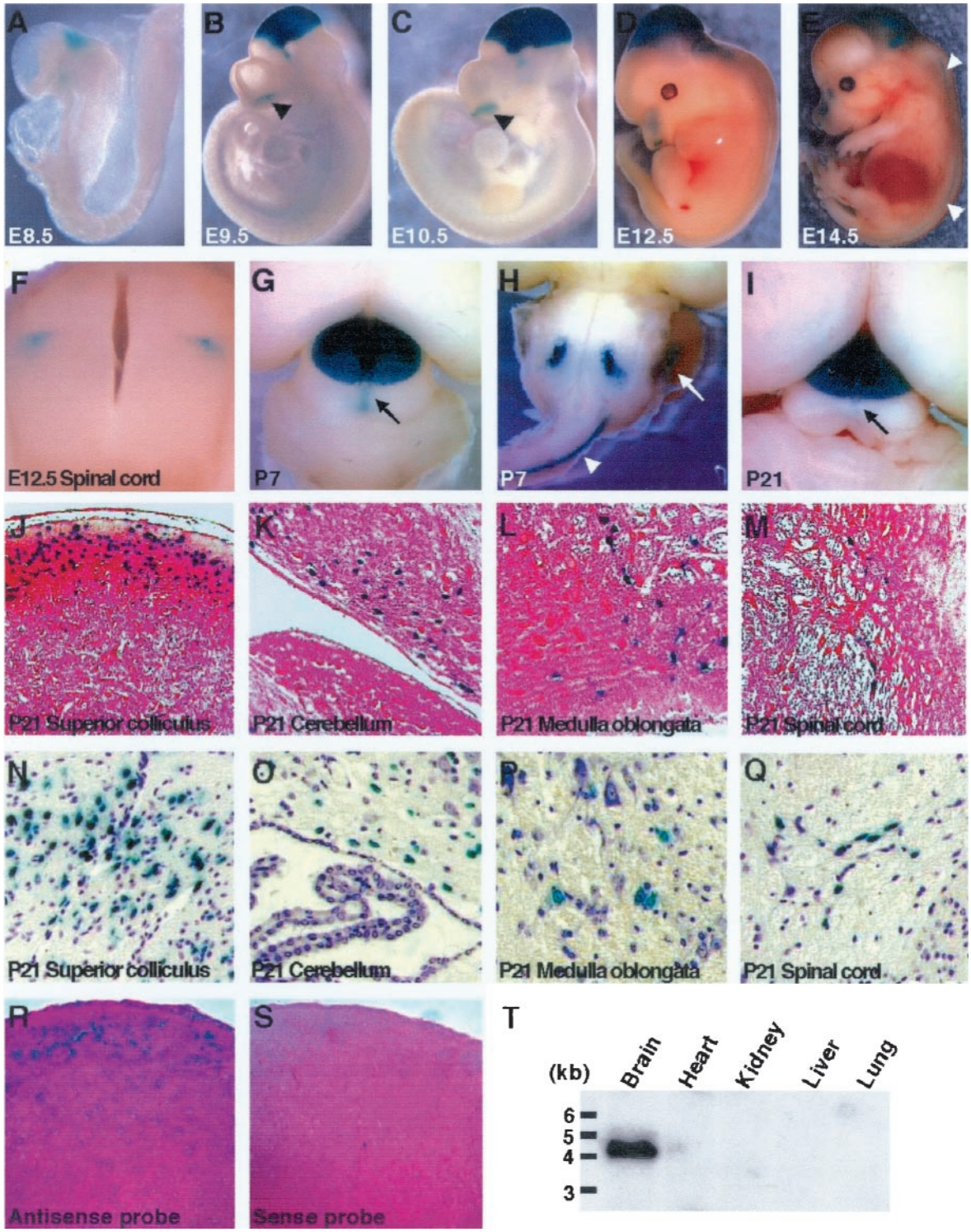

FIG. 2. (A to Q) X-Gal (5-bromo-4-chloro-3-indolyl-β-D-galactopyranoside) staining of *Dmbx1*^{z} heterozygous mutant mice. The solid and open arrowheads indicate the nasal pit and spinal cord, respectively. The solid and open arrows indicate the inferior colliculus and cerebellum, respectively. (R and S) In situ hybridization of *Dmbx1*. (T) Northern analysis of adult tissues. (A) E8.5. (B) E9.5. (C) E10.5. (D) E12.5. (E) E14.5. (F) Cross-section of E12.5 spinal cord. (G) Dorsal view of P7 brain. (H) Ventral view of P7 brain. (I) Dorsal view of P21 brain. (J to M) X-Gal and eosin Y costained paraffin sections. The blue cells are *Dmbx1-lacZ*-positive cells. (N to Q) X-Gal- and cresyl violet-costained paraffin sections. (R and S) Superior colliculus of postnatal brain counterstained with eosin Y.

TABLE 1. Summary of *Dmbx1* heterozygous intercrosses

Mutant	Stage	No. (%)					Total	Avg litter size
		+/+	+/−	−/−	+/z	−/z		
Dmbx1$^{+/-}$	E 18.5	13 (27.1)	22 (45.8)	13 (27.1)			48	6.0
	P9[a]	47 (32.2)	80 (54.8)	19 (13.0)			146	7.7
Dmbx1$^{z/+}$	P9[a]	47 (38.5)			63 (51.6)	12 (9.8)	122	7.2

[a] $P < 0.01$ (chi-square test).

homozygous mutant mice after birth, suggesting that impaired milk intake caused the neonatal lethality and poor growth (Fig. 3D). Because it is well known that pituitary deficiency can result in growth deficiency, we examined the expression of GH and TSH by immunohistochemistry (Fig. 3E). GH and TSH immunostaining was detected in the pituitary glands of *Dmbx1*$^{-/-}$ mice.

Aberrant expression of *Dmbx1-lacZ* in *Dmbx1* mutant mice. We next examined *Dmbx1-lacZ* expression in *Dmbx1* mutant mice. To control for the number of *lacZ* alleles used, we compared *lacZ* expression levels in *Dmbx1*$^{z/+}$ and *Dmbx1*$^{z/-}$ mice. At P7, the *Dmbx1-lacZ*-expressing region in the inferior colliculus was expanded in *Dmbx1*$^{z/-}$ in comparison to *Dmbx1*$^{z/+}$ mice (Fig. 4A and B). On the other hand, the number of *Dmbx1-lacZ*-expressing cells in the ventral region of the medulla oblongata was reduced in *Dmbx1*$^{z/-}$ mice (Fig. 4C and D). These observations were also found at P1 and P14, suggesting that the aberrant expression of *Dmbx1-lacZ* was maintained throughout the neonatal period (Fig. 4E to H and data not shown). Histological analysis of serial sections of P21 brains revealed that a substantial number of *lacZ*-positive cells were observed in the inferior colliculus in *Dmbx1*$^{z/-}$ mice, while no *LacZ*-positive cells were detected in *Dmbx1*$^{z/+}$ mice (Fig. 4I and J). In the cerebellum, the number of *lacZ*-expressing deep nuclei was reduced in *Dmbx1*$^{z/-}$ mice compared to *Dmbx1*$^{z/+}$ mice, and the ratio of *lacZ*-positive cells per section was 1:0.24 ($P < 0.001$; *t* test) (Fig. 4K and L). In the ventral region of the medulla oblongata, the *lacZ*-expressing cells were also reduced in number, and the ratio was 1:0.45 ($P < 0.001$; *t* test) (Fig. 4M and N). Since the aberrant expression of *Dmbx1-lacZ* was noticed at P1, we also examined *Dmbx1-lacZ* expression during embryonic stages. At E9.5 and E11.5, the regions that express *lacZ* were comparable between *Dmbx1*$^{z/+}$ and *Dmbx1*$^{z/-}$ embryos; however, the intensity of the staining was stronger in *Dmbx1*$^{z/-}$ embryos than in *Dmbx1*$^{z/+}$ embryos (Fig. 4O to R). In spite of this difference in *Dmbx1-lacZ* expression, overall brain structure was maintained in *Dmbx1*$^{z/-}$ embryos, and no obvious defects were observed at E9.5 or E10.5 using a *Phox2* probe as an early marker for catecholaminergic neurons or antineurofilament staining, respectively (Fig. 4S and T and data not shown).

Nursing defect of *Dmbx1* mutant mice. We next examined the phenotypes of mature *Dmbx1* homozygous mutant mice. Both male and female *Dmbx1* homozygous mutant mice were fertile. However, while breeding *Dmbx1* homozygous mutant mice, we noticed that the number of surviving offspring from *Dmbx1* homozygous mutant females was lower than that from *Dmbx1* heterozygous mutant females (Table 2). When we crossed *Dmbx1*$^{-/-}$ males to *Dmbx1*$^{+/-}$ females, most of the *Dmbx1*$^{+/-}$ pups survived to P21. However, ~50% of the *Dmbx*$^{-/-}$ mice died during the neonatal period, confirming the neonatal lethality of *Dmbx1* mutant mice. When we crossed *Dmbx1*$^{+/-}$ males to *Dmbx1*$^{-/-}$ females, even the percentage of *Dmbx1*$^{+/-}$ pups was reduced, and the *Dmbx1*$^{-/-}$ pups rarely survived to P21. Interestingly, *Dmbx1*$^{+/-}$ pups raised by *Dmbx1*$^{-/-}$ females grew poorly and were similar in weight to *Dmbx1*$^{-/-}$ pups nursed by *Dmbx1*$^{+/-}$ females (Fig. 5A). The growth defect was not due to the genotypes of the pups, because growth impairment was observed even when wild-type pups were cross-fostered to *Dmbx1*$^{-/-}$ females (Fig. 5B). These observations indicate that *Dmbx1*$^{-/-}$ females have a nursing defect. Maternal behaviors, such as nest building and pup retrieval, seemed normal in *Dmbx1*$^{-/-}$ females, and they did not abandon their pups (data not shown). We also examined the mammary glands of postpartum *Dmbx1*$^{-/-}$ females (Fig. 5C). Milk production was clearly evident, and well-differentiated duct formation was detected in *Dmbx1*$^{-/-}$ females.

DISCUSSION

To investigate the in vivo role of *Dmbx1*, we generated *Dmbx1* mutant mice. The *Dmbx1*^{z} allele recapitulated the previously reported *Dmbx1* mRNA expression patterns during embryonic stages and identified several sites in the postnatal CNS as potential *Dmbx1*-expressing regions. After birth, *Dmbx1-lacZ* expression was detected in subpopulations of the superior colliculus, inferior colliculus, medulla oblongata, cerebellum, and spinal cord. These observations suggest that *Dmbx1* is expressed postnatally in the CNS and marks a unique population of neuronal cells. The *Dmbx1-lacZ* expression in the postnatal brain was confirmed by section in situ hybridization and Northern analysis of *Dmbx1* mRNA. The numbers of *Dmbx1-lacZ*-expressing cells in the inferior colliculus were gradually reduced during the neonatal period, indicating that the expression of *Dmbx1* is temporally and spatially regulated or that *Dmbx1*-expressing neurons are progressively lost after birth.

Although *Dmbx1* is expressed in the forebrain, midbrain, and hindbrain during embryogenesis, *Dmbx1* homozygous mutant mice were born without any overt alterations in brain structure. This is in contrast to other homeobox genes that are expressed in embryonic brains, such as *Otx2*, *En1*, and *Gbx2*. *Otx2* homozygous mutant mice lack rostal brain structures, and both midbrain and rostal hindbrain tissue is missing in *En1* homozygous mutant mice (1, 3, 17, 18, 30, 37). *Gbx2* is required for the development of the midbrain-hindbrain junction (34). A previous report suggested that *Otx2* is necessary for the expression of *Dmbx1* in the midbrain (16). However, the phenotypes of *Otx2* mutant mice are not due only to the loss of *Dmbx1*, because *Dmbx1* mutant mice have overtly normal

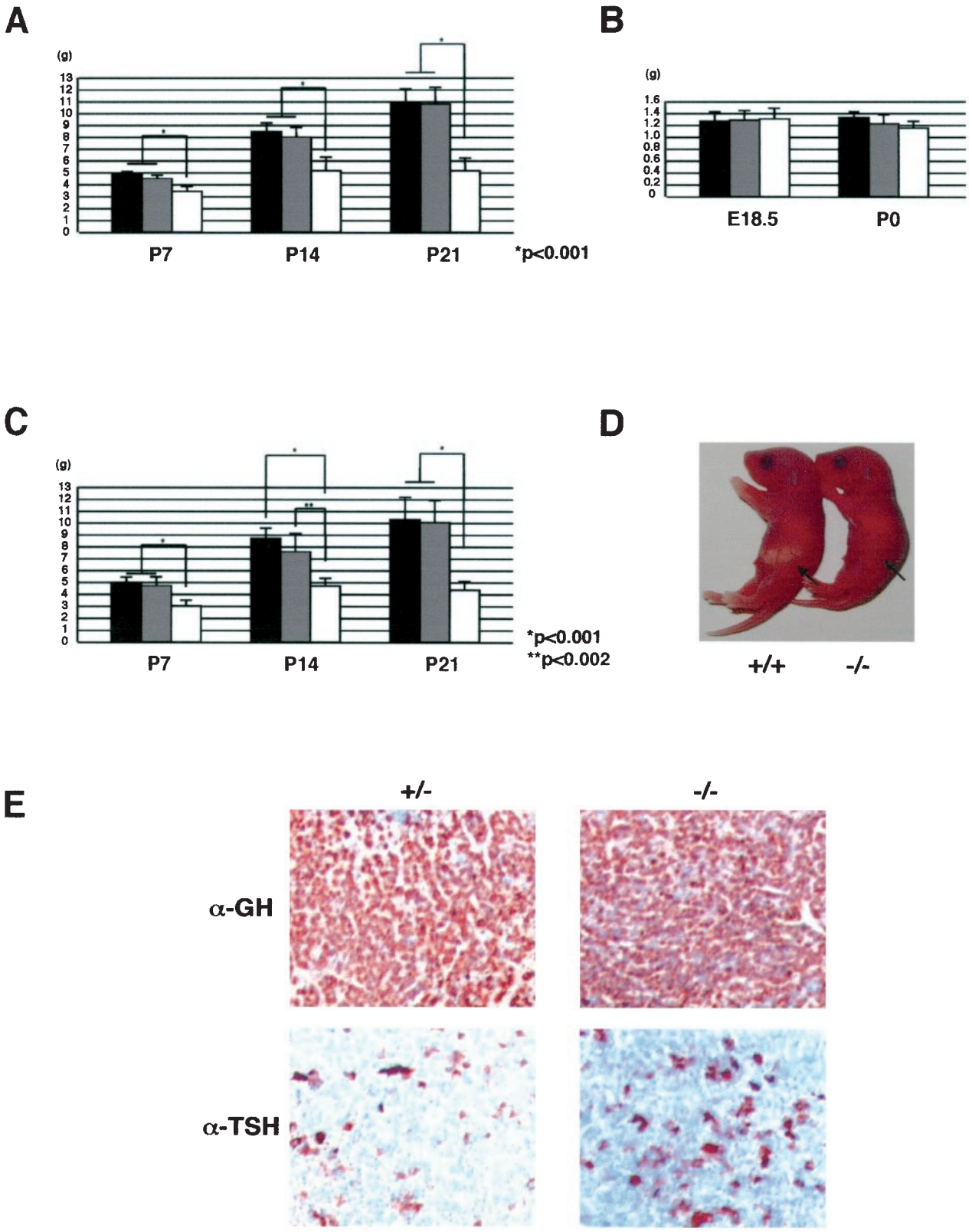

FIG. 3. (A) Body weights of wild-type (solid bars; $n = 9$ for P7, 8 for P14, and 10 for P21), *Dmbx1*$^{+/-}$ (shaded bars; $n = 8$ for P7, 14 for P14, and 8 for P21), and *Dmbx1*$^{-/-}$ (open bars; $n = 8$ for P7, 12 for P14, and 12 for P21) mice. Standard deviations are indicated by the error bars. Statistical analyses were scored by *t* test. (B) Body weights of wild-type (solid bars; $n = 8$ for E18.5 and 9 for P0), *Dmbx1*$^{+/-}$ (shaded bars; $n = 14$ for E18.5 and 8 for P0), and *Dmbx1*$^{-/-}$ (open bars; $n = 10$ for E18.5 and 9 for P1) mice. (C) Body weights of wild-type (solid bars; $n = 5$ for P7, 4 for P14, and 5 for P21), *Dmbx1*$^{z/+}$ (shaded bars; $n = 7$ for P7, 5 for P14, and 8 for P21), and *Dmbx1*$^{z/z}$ (open bars; $n = 7$ for P7, 4 for P14, and 7 for P21) mice. Statistical analyses were scored by *t* test. (D) Appearance of neonates (P0). +/+, wild type; −/−, *Dmbx1*$^{-/-}$ littermate. The arrows indicate the positions of the stomachs. (E) Immunohistochemistry of pituitary glands at P21. +/−, *Dmbx1*$^{+/-}$ mice; −/−, *Dmbx1*$^{-/-}$ mice. α-GH, anti-GH; α-TSH, anti-TSH.

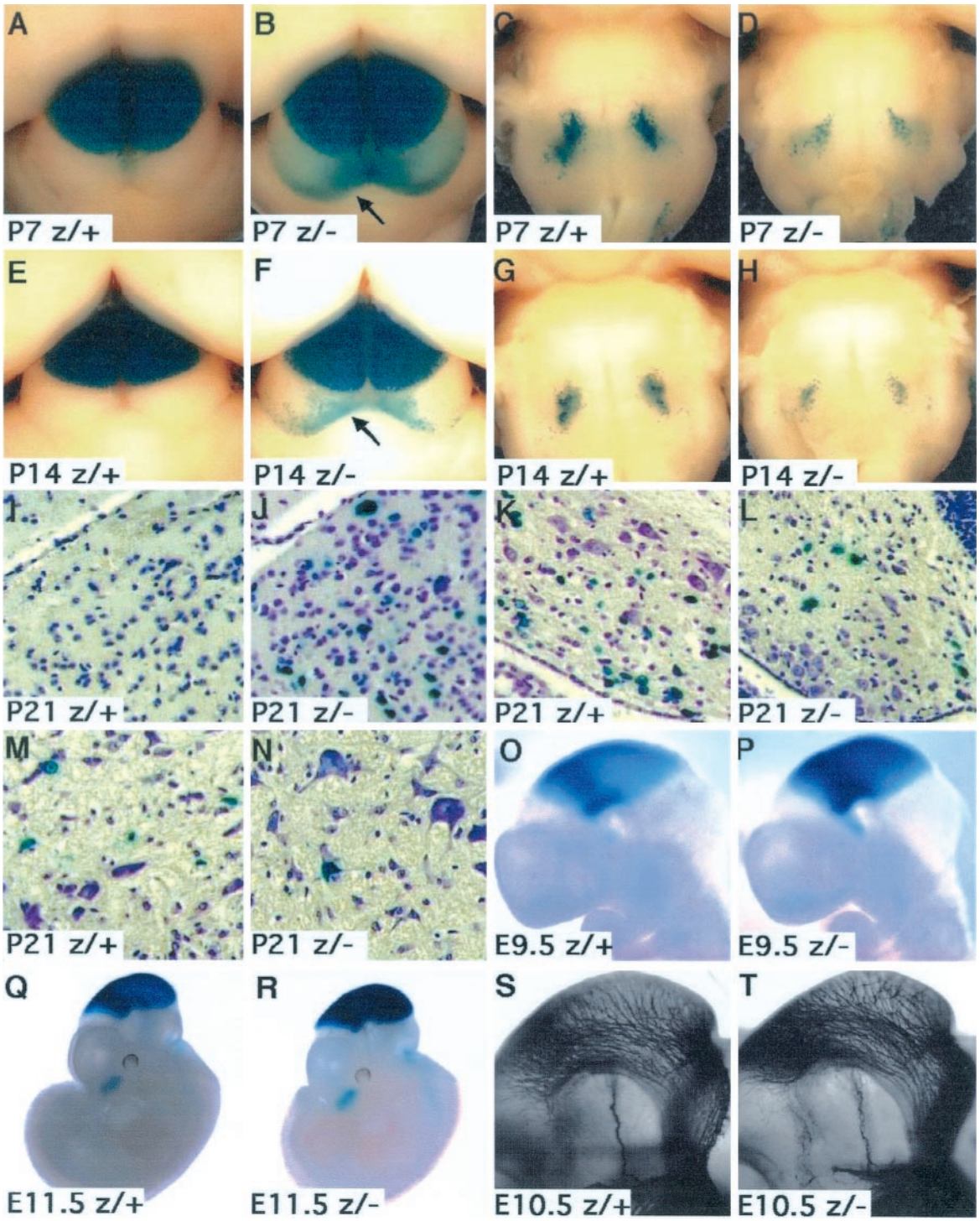

FIG. 4. Comparison of *Dmbx1-lacZ* expression (A to R) and anti-neurofilament staining (S and T). (A and B) Dorsal views of P7 brains. (C and D) Ventral views of P7 brains. (E and F) Dorsal views of P14 brains. (G and H) Ventral views of P14 brains. (I to N) X-Gal- and cresyl violet-costained paraffin sections of P21 brains. (I and J) Inferior colliculus. (K and L) Cerebellum. (M and N) Ventral regions of medulla oblongata. (O and P) E9.5. (Q and R) E11.5. (S and T) E10.5. The arrows in panels B and F indicate the *Dmbx1-lacZ*-positive cells in the inferior colliculus. (A, C, E, G, I, K, M, O, Q, and S) $Dmbx1^{z/+}$. (B, D, F, H, J, L, N, P, R, and T) $Dmbx1^{z/-}$.

brains and *Dmbx1* is dispensable for survival during embryogenesis.

Although *Dmbx1* homozygous mutant mice manifested no obvious malformations of the brain, they appeared to have abnormalities in the development of cell lineages in the CNS, because $Dmbx1^{z/-}$ mice exhibited aberrant *Dmbx1-lacZ* expression patterns. *Dmbx1-lacZ*-expressing cells in deep nuclei of the cerebellum and the ventral region of the medulla ob-

TABLE 2. Survival of pups fostered by *Dmbx1*$^{-/-}$ mice

Genotype of parents (female × male)	No. of litters	No. of pups of genotype:					
		+/−			−/−		
		P0	P21	Ratio[a] (%)	P0	P21	Ratio[a]
+/− × −/−	8	31	30	97	35	19	54
−/− × +/−	7	27	16	59	13	0	0

[a] Survival ratio (P21/P0).

longata were reduced in number, while in the inferior colliculus, an increased number of *Dmbx1-lacZ*-expressing cells were detected at birth and through the neonatal period. These observations suggest that *Dmbx1* is required for the proper generation or function of specific cell populations in the CNS.

We compared the *Dmbx1-lacZ* expression patterns during embryogenesis and noticed that the intensity of the *lacZ* staining was stronger in *Dmbx1*$^{z/-}$ than *Dmbx1*$^{z/+}$ embryos at E9.5 and E11.5. However, the regions that express *Dmbx1-lacZ* were comparable in *Dmbx1*$^{z/-}$ and *Dmbx1*$^{z/+}$ embryos, with a sharp boundary between the midbrain and the midbrain-hindbrain junction at E9.5. These observations indicate that *Dmbx1* has an autoregulatory mechanism to down-regulate its expression; however, the autoregulation is dispensable for the boundary formation of *Dmbx1*-expressing compartments. Previously it was reported that *Dmbx1* expression was suppressed by *Gbx2* in the midbrain-hindbrain junction (16). Thus, our results suggest that the repression of *Dmbx1* expression by GBX2 occurs independently of DMBX1.

Several *Dmbx1* homozygous mutant mice were found dead within 24 h after birth without milk in their stomachs. Once they suckled, they survived for at least several days, although some of them died before being weaned, gradually losing weight. These observations support the possibility that there is a *Dmbx1*-dependent impairment of milk intake that causes mortality during the neonatal period. It is likely that the milk intake deficit also influences growth, because all of the *Dmbx1* homozygous mutant mice manifested a growth defect. The growth retardation was noticed within 3 days after birth, and this is in contrast to dwarfisms caused by pituitary deficiencies, in which growth defects are usually detected 1 week after birth. Hypogonadal and hypothyroid mice lacking the common α subunit of TSH, luteinizing hormone, and follicle-stimulating hormone demonstrate apparently reduced growth between 2 and 3 weeks of age (11). *Otx1*-null mice, which manifest low levels of GH, follicle-stimulating hormone, and luteinizing hormone, exhibit dwarfism around P7 (2). Laron-type dwarfisms, which are caused by GH insensitivity, also exhibit significant weight differences after the first week of life (26, 38). We have not observed any skeletal abnormalities in *Dmbx1* mutant mice, such as tail kinks or bends, rounded heads, or misaligned teeth, which are characteristics of *Fgfr3* mutant dwarf mice (6, 33). These findings, in conjunction with the observation that the production of GH and TSH is maintained in the pituitary glands of *Dmbx1* homozygous mutant mice, suggest that the growth defects were caused by insufficient milk intake and were not due to pituitary dysfunction or skeletal dysplasia. The abnormal development of the CNS seems to be related to the deficit of milk intake in *Dmbx1* mutant mice.

The body weights of adult *Dmbx1* homozygous mutant mice never catch up with those of wild-type or *Dmbx1* heterozygous littermates, and in most cases, the homozygous mutant mice are 20 to 50% lighter in weight than the others. Nevertheless, the responses to starvation stress of adult *Dmbx1*$^{-/-}$ mice were virtually normal. They lost and gained weight as much as *Dmbx1*$^{+/-}$ mice after a 24-h starvation and refeeding, respectively (data not shown). The recovery of body weight was due to hyperphagia, and *Dmbx1*$^{-/-}$ mice ate more during the first day of refeeding than the second day, like *Dmbx1*$^{+/-}$ mice (data not shown). These observations indicate that adult *Dmbx1* homozygous mutant mice manifest normal eating behaviors. The reduced body weight of adult *Dmbx1* homozygous mutant mice can be attributed to insufficient milk intake prior to weaning, because an increased growth rate was observed after weaning in *Dmbx1* homozygous mutant mice, like wild-type and *Dmbx1* heterozygous mutant mice.

Both male and female *Dmbx1* homozygous mutant mice were fertile. However, pups from *Dmbx1* homozygous mutant females showed a high mortality ratio compared to pups from *Dmbx1* heterozygous mutant females. Furthermore, the surviving pups manifested the growth impairment even if they were *Dmbx1* heterozygotes. These phenotypes did not depend on the genotypes of the pups or the sizes of litters and were caused by a maternal defect, because similar results were obtained when wild-type pups were cross-fostered by *Dmbx1* homozygous mutant females. It was previously reported that deficits of maternal behaviors can cause lethality or growth defects in offspring. *fosB* mutant mice are deficient in retrieval responses and crouching behaviors, and most pups die within 2 days after birth (5). Two imprinted genes, *Mest* and *Peg3*, are related to maternal behaviors, and heterozygous mutant mice are defective in nursing and their offspring are growth impaired and show a low survival rate (14, 15). *Mbd2* homozygous mutant mice show poor retrieval responses, and their pups are growth retarded (9). *Dbh*-deficient mice, which lack the enzyme responsible for the synthesis of (nor)epinephrine, manifest impaired maternal behaviors, and their pups die within several days after birth (31). In *Dmbx1* homozygous mutant mice, the expression of TH, the enzyme essential for the synthesis of dopamine and (nor)epinephrine, was detected by immunohistochemistry, and *Dmbx1-lacZ*-expressing cells are noncatecholaminergic neurons (data not shown). We have also observed normal maternal behaviors, such as nest building and pup retrieval, in *Dmbx1* homozygous mutant females. Hence, the growth impairment and lethality in pups nursed by *Dmbx1* homozygous mutant females are not likely caused by deficits of maternal behavior.

Although oxytocin-deficient mice exhibit normal maternal behaviors, their pups die within 24 h of delivery with no milk in their stomachs (21). Offspring of *Id2* homozygous mutant mothers die within 2 days after birth due to a lactation defect (19). Examination of the mammary glands of postpartum *Dmbx1* homozygous mutant females revealed well-differentiated duct formation and milk accumulation. Therefore, an impaired milk ejection reflex may be responsible for the neonatal lethality and growth defects in pups nursed by *Dmbx1* homozygous mutant females.

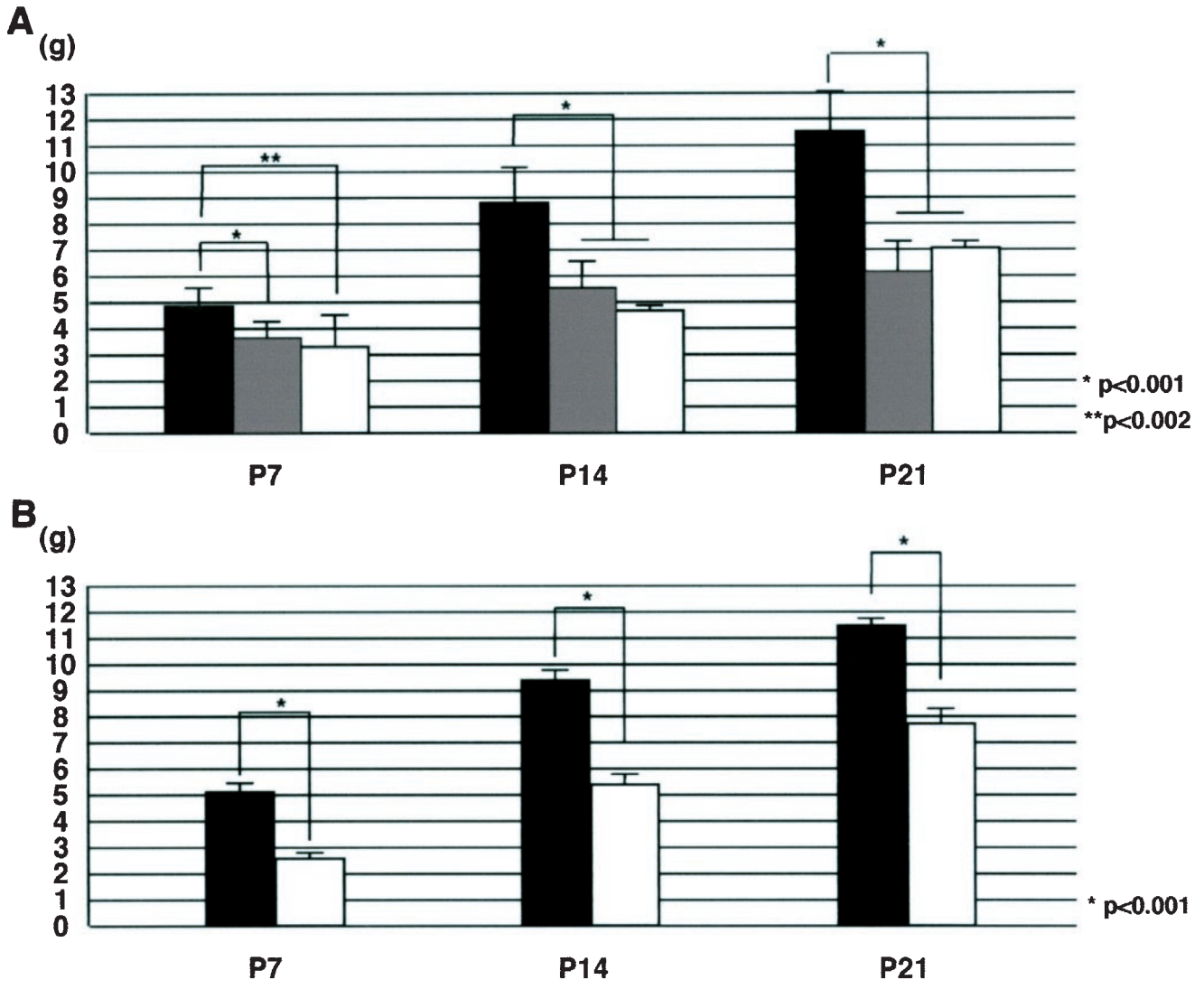

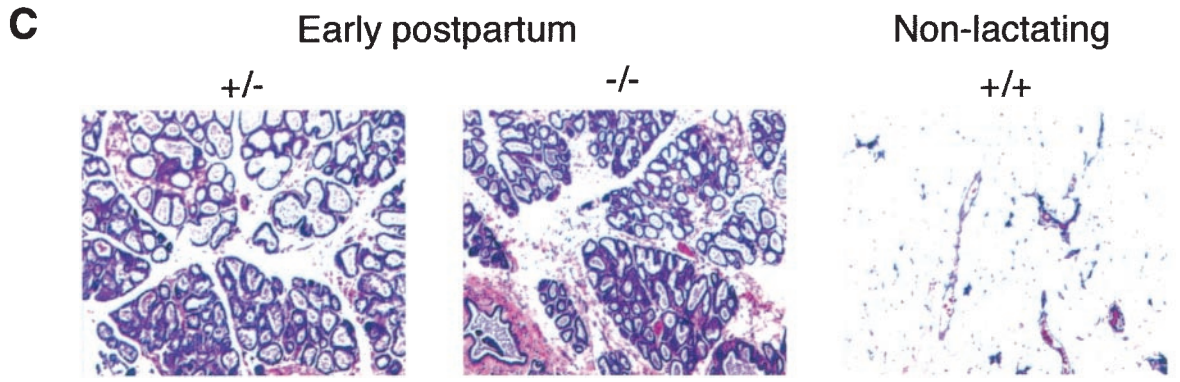

FIG. 5. (A) Body weights of *Dmbx1*$^{+/-}$ pups nursed by *Dmbx1*$^{+/-}$ females (solid bars; $n = 14$ for P7, 14 for P14, and 22 for P21), *Dmbx1*$^{-/-}$ pups nursed by *Dmbx1*$^{+/-}$ females (shaded bars; $n = 11$ for P7, 10 for P14, and 15 for P21), and *Dmbx1*$^{-/-}$ pups nursed by *Dmbx1*$^{-/-}$ females (open bars; $n = 9$ for P7, 6 for P14, and 6 for P21). Standard deviations are indicated by the error bars. Statistical analyses were scored by *t* test. (B) Body weights of wild-type pups cross-fostered by *Dmbx1*$^{+/-}$ females (solid bars; $n = 5$) and wild-type pups cross-fostered by *Dmbx1*$^{-/-}$ females (open bars; $n = 4$). Statistical analyses were scored by *t* test. (C) Histological examinations of mammary glands. Paraffin sections were stained by hematoxylin and eosin Y. +/+, wild-type; +/−, *Dmbx1*$^{+/-}$; −/−, *Dmbx1*$^{-/-}$ females.

It is interesting that *Foxb1* (a winged helix gene)-deficient mice share some phenotypes with *Dmbx1* mutant mice (7, 13, 35). *Foxb1* mutant mice are postnatally growth retarded, which is noticeable within 2 to 3 days after birth, and remain proportionally smaller in adulthood, although the growth curve is parallel to that of wild-type or heterozygous animals. Thirty to 50% of *Foxb1* mutant mice die before being weaned, and the peak of lethality is observed in the first 2 days after birth. They have normal circulating GH and TSH, and the growth retardation is not due to a pituitary deficiency. Surviving *Foxb1* mutant mice are fertile, but *Foxb1* mutant females have a defect in the milk ejection reflex. Thus, we examined *Foxb1* expression in the neural tissues of *Dmbx1* mutant mice during embryogenesis and after birth (data not shown). However, we found no differences in *Foxb1* expression, suggesting that *Foxb1* does not mediate the *Dmbx1* mutant phenotype. It was proposed that morphological defects in the inferior colliculi were responsible for the lactation defect of *Foxb1* mutant mice (12). This proposal suggests a similar cause for the *Dmbx1* maternal phenotypes, since an aberrant expression of *Dmbx1-lacZ* was observed in the inferior colliculus in *Dmbx1* mutant mice. Determining the neuronal networks mediated by *Dmbx1*-expressing neurons will be useful for understanding the phenotypes of mutant mice.

In summary, we have demonstrated that *Dmbx1* is expressed in the neuronal tissues during both the embryonic and postnatal periods and is required for survival, growth, normal brain development, and maternal activity in mice. Since the sequence of *Dmbx1* is highly conserved between mouse and human (24), the impaired function of human DMBX1 might be related to neurological disorders, such as impaired food intake and milk ejection reflex, that are relevant to the phenotype of *Dmbx1* mutant mice.

ACKNOWLEDGMENTS

These studies were supported by Public Health Service grant HD30284 from the National Institutes of Health (NIH) to R.R.B. DNA sequencing and veterinary resources were supported by NIH Cancer Center Support (Core) Grant CA16672.

All research complied with all relevant federal guidelines and institutional policies.

We thank Steve O'Gorman for PC3 ES cells, Allan Bradley for SNL 76/7 STO cells, Jenny Deng for assistance with tissue culture, Ying Wang for immunohistochemistry, and Dawna Armstrong and Randy Johnson for helpful discussions.

REFERENCES

1. **Acampora, D., S. Mazan, Y. Lallemand, V. Avantaggiato, M. Maury, A. Simeone, and P. Brûlet.** 1995. Forebrain and midbrain regions are deleted in *Otx2*$^{-/-}$ mutants due to a defective anterior neuroectoderm specification during gastrulation. Development **121:**3279–3290.
2. **Acampora, D., S. Mazan, F. Tuorto, V. Avantaggiato, J. J. Tremblay, D. Lazzaro, A. di Carlo, A. Mariano, P. E. Macchia, G. Corte, V. Macchia, J. Drouin, P. Brûlet, and A. Simeone.** 1998. Transient dwarfism and hypogonadism in mice lacking *Otx1* reveal prepubescent stage-specific control of pituitary levels of GH, FSH and LH. Development **125:**1229–1239.
3. **Ang, S.-L., O. Jin, M. Rhinn, N. Daigle, L. Stevenson, and J. Rossant.** 1996. A targeted mouse *Otx2* mutation leads to severe defects in gastrulation and formation of axial mesoderm and to deletion of rostal brain. Development **122:**243–252.
4. **Broccoli, V., E. Colombo, and G. Cossu.** 2002. *Dmbx1* is a paired-box containing gene specifically expressed in the caudal most brain structures. Mech. Dev. **114:**219–223.
5. **Brown, J. R., H. Ye, R. T. Bronson, P. Dikkes, and M. E. Greenberg.** 1996. A defect in nurturing in mice lacking the immediate early gene *fosB*. Cell **86:**297–309.
6. **Colvin, J. S., B. A. Bohne, G. W. Harding, D. G. McEwen, and D. M. Ornitz.** 1996. Skeletal overgrowth and deafness in mice lacking fibroblast growth factor receptor 3. Nat. Genet. **12:**390–397.
7. **Dou, C., X. Ye, C. Stewart, E. Lai, and S. C. Li.** 1997. TWH regulates the development of subsets of spinal cord neurons. Neuron **18:**539–551.
8. **Gogoi, R. N., F. R. Schubert, J.-P. Martinez-Barbera, D. Acampora, A. Simeone, and A. Lumsden.** 2002. The paired-type homeobox gene Dmbx1 marks the midbrain and tectum. Mech. Dev. **114:**213–217.
9. **Hendrich, B., J. Guy, B. Ramsahoye, V. A. Wilson, and A. Bird.** 2001. Closely related proteins MBD2 and MBD3 play distinctive but interacting roles in mouse development. Genes Dev. **15:**710–723.
10. **Kawahara, A., C.-B. Chien, and I. B. Dawid.** 2002. The homeobox gene mbx1 is involved in eye and tectum development. Dev. Biol. **248:**107–117.
11. **Kendall, S. K., L. C. Samuelson, T. L. Saunders, R. I. Wood, and S. A. Camper.** 1995. Targeted disruption of the pituitary glycoprotein hormone α-subunit produces hypogonadal and hypothyroid mice. Genes Dev. **9:**2007–2019.
12. **Kloetzli, J. M., I. A. Fontaine-Glover, E. R. Brown, M. Kuo, and P. A. Labosky.** 2001. The winged helix gene, Foxb1, controls development of mammary glands and regions of the CNS that regulate the milk-ejection reflex. Genesis **29:**60–71.
13. **Labosky, P. A., G. E. Winnier, T. L. Jetton, L. Hargett, A. K. Ryan, M. G., Rosenfeld, A. F. Parlow, and B. L. Hogan.** 1997. The winged helix gene, Mf3, is required for normal development of the diencephalon and midbrain, postnatal growth and the milk-ejection reflex. Development **124:**1263–1274.
14. **Lefebvre, L., S. Viville, S. C. Barton, F. Ishino, E. B. Keverne, and M. A. Surani.** 1998. Abnormal maternal behaviour and growth retardation associated with loss of the imprinted gene *Mest*. Nat. Genet. **20:**163–169.
15. **Li, L.-L., E. B. Keverne, S. A. Aparicio, F. Ishino, S. C. Barton, and M. A. Surani.** 1999. Regulation of maternal behavior and offspring growth by paternally expressed Peg3. Science **284:**330–333.
16. **Martinez-Barbera, J. P., M. Signore, P. P. Boyl, E. Puelles, D. Acampora, R. Gogoi, F. Schubert, A. Lumsden, and A. Simeone.** 2001. Regulation of anterior neuroectoderm and its competence in responding to forebrain and midbrain inducing activities depend on mutual antagonism between OTX2 and GBX2. Development **128:**4789–4800.
17. **Matsuo, I., S. Kuratani, C. Kimura, N. Takeda, and S. Aizawa.** 1995. Mouse *Otx2* functions in the formation and patterning of rostal head. Genes Dev. **9:**2646–2658.
18. **McMahon, A. P., and A. Bradley.** 1990. The *Wnt*-1 (*int*-1) proto-oncogene is required for development of a large region of the mouse brain. Cell **62:**1073–1085.
19. **Mori, S., S.-I. Nishikawa, and Y. Yokota.** 2000. Lactation defect in mice lacking the helix-loop-helix inhibitor Id2. EMBO J. **19:**5772–5781.
20. **Morin, X., H. Cremer, M.-R. Hirsch, R. P. Kapur, C. Goridis, and J.-F. Brunet.** 1997. Defect in sensory and autonomic ganglia and absence of locus coeruleus in mice deficient for the homeobox gene *Phox2a*. Neuron **18:**411–423.
21. **Nishimori, K., L. J. Young, Q. Guo, Z. Wang, T. R. Insel, and M. M. Matzuk.** 1996. Oxytocin is required for nursing but is not essential for parturition or reproductive behavior. 1996. Proc. Natl. Acad. Sci. USA **93:**11699–11704.
22. **O'Gorman, S., N. A. Dagenais, M. Qian, and Y. Marchuk,.** 1997. Protamine-Cre recombinase transgenes efficiently recombine target sequences in the male germ line of mice, but not in embryonic stem cells. Proc. Natl. Acad. Sci. USA **94:**14602–14607.
23. **Ohtoshi, A., M. J. Justice, and R. R. Behringer.** 2001. Isolation and characterization of *Vsx1*, a novel mouse CVC *paired-like* homeobox gene expressed during embryogenesis and retina. Biochem. Biophys. Res. Commun. **286:**133–140.
24. **Ohtoshi, A., I. Nishijima, M. J. Justice, and R. R. Behringer.** 2002. *Dmbx1*, a novel evolutionarily conserved *paired*-like homeobox gene expressed in the brain of mouse embryos. Mech. Dev. **110:**241–244.
25. **Pattyn, A., X. Morin, H. Cremer, C. Goridis, and J.-F. Brunet.** 1999. The homeobox gene *Phox2b* is essential for the development of autonomic neural crest derivatives. Nature **399:**366–370.
26. **Pontoglio, M., J. Barra, M. Hadchouel, A. Doyen, C. Kress, J. P. Bach, C. Babinet, and M. Yaniv.** 1996. Hepatocyte nuclear 1 inactivation results in hepatic dysfunction, phenylketonuria, and renal Fanconi syndrome. Cell **84:**575–585.
27. **Rubenstein, J. L. R., S. Martinez, K. Shimamura, and L. Puelles.** 1994. The embryonic vertebrate forebrain: the prosomeric model. Science **266:**578–580.
28. **Rubenstein, J. L. R., K. Shimamura, S. Martinez, and L. Puelles.** 1998. Regionalization of the prosencephalic neural plate. Annu. Rev. Neurosci. **21:**445–477.
29. **Sornson, M. W., W. Wu, J. S. Dasen, S. E. Flynn, D. J. Norman, S. M. O'Connell, I. Gukovsky, C. Carrière, A. K. Ryan, A. P. Miller, L. Zuo, A. S. Gleibermann, B. Andersen, W. G. Beamer, and M. G. Rosenfeld.** 1996. Pituitary lineage determination by the *Prophet of Pit-1* homeodomain factor defective in Ames dwarfism. Nature **384:**327–333.
30. **Thomas, K. R., and M. R. Capecci.** 1990. Targeted disruption of the murine *int-1* proto-oncogene resulting in severe abnormalities in midbrain and cerebellar development. Nature **346:**847–850.

31. **Thomas, S. A., and R. D. Palmiter.** 1997. Impaired maternal behavior in mice lacking norepinephrine and epinephrine. Cell **91:**583–592.
32. **Vollmer, J.-Y., and R. G. Clerc.** 1998. Homeobox genes in the developmental mouse brain. J. Neurochem. **71:**1–19.
33. **Wang, Y., M. K. Spatz, K. Kannan, H. Hayk, A. Avivi, M. Gorivodsky, M. Pines, A. Yayon, P. Lonai, and D. Givol.** 1999. A mouse model for achondroplasia produced by targeting fibroblast growth factor receptor 3. Proc. Natl. Acad. Sci. USA **96:**4455–4460.
34. **Wassarmann, K. M., M. Lewandoski, K. Campbell, A. L. Joyner, J. L. R. Rubenstein, S. Martinez, and G. R. Martin.** 1997. Specification of the anterior hindbrain and establishment of a normal mid/hindbrain organizer is dependent on *Gbx2* gene function. Development **124:**2923–2934.
35. **Wehr, R., A. Mansouri, T. de Maeyer, and P. Gruss.** 1997. *Fkh5*-deficient mice slow dysgenesis in the caudal midbrain and hypothalamic mammillary body. Development **124:**4447–4456.
36. **Weimann, J. M., Y. A. Zhang, M. E. Levin, W. P. Devine, P. Brûlet, and S. K. McConnell.** 1999. Cortical neurons require Otx1 for the refinement of exuberant axonal projections to subcortical targets. Neuron **24:**819–831.
37. **Wurst, W., A. B. Auerbach, and A. L. Joyner.** 1994. Multiple development defects in *Engrailed-1* mutant mice: an early mid-hindbrain deletion and patterning defects in forelimbs and sternum. Development **120:**2065–2075.
38. **Zhou, Y., B. C. Xu, H. G. Maheshwari, L. He, M. Reed, M. Lozykowski, S. Okada, L. Cataldo, K. Coschigamo, T. E. Wagner, G. Baumann, and J. J. Kopchick.** 1997. A mammalian model for Laron syndrome produced by targeted disruption of the mouse GH receptor/binding protein gene (the Laron mouse). Proc. Natl. Acad. Sci. USA **94:**13215–13220.